Available online at www.sciencedirect.com
ScienceDirect
Journal of Physics and Chemistry of Solids 68 (2007) 290–298
JOURNAL OF PHYSICS AND CHEMISTRY OF SOLIDS
www.elsevier.com/locate/jpcs

Mixed valence states in cobalt iron cyanide

R. Martínez-García[a], M. Knobel[b], J. Balmaseda[a,c], H. Yee-Madeira[d,1], E. Reguera[a,e,*,1]

[a]*Institute of Materials Science and Technology, University of Havana, 10400 Havana, Cuba*
[b]*Institute of Physics "Gleb Wataghin", UNICAMP, Campinas, Brazil*
[c]*Institute of Materials Research, UNAM, Mexico, D.F.*
[d]*School of Physics and Mathematics of IPN, Mexico, D.F.*
[e]*Centre for Applied Science and Advanced Technology of IPN, Mexico, D.F.*

Received 10 May 2006; received in revised form 5 November 2006; accepted 15 November 2006

Abstract

Cobalt iron cyanide with both Co and Fe in mixed valence states were prepared and characterized. In this mixed valence system the cobalt atom is found both as high spin Co(2+) and low spin Co(III) while iron always appears in low spin state to form two solid solutions: Co(2+)Co(III) hexacyanoferrates (II,III), and Co(2+)Co(III) hexacyanoferrate (II). Such solid solutions have the following formula units: $(Co^{2+})_x(Co^{III})_{1-x}K[(Fe^{II})_{1-x}(Fe^{III})_x(CN)_6]\cdot\frac{1}{2}H_2O$ and $(Co^{2+})_{1.5x}(Co^{III})_{1-x}K[Fe^{II}(CN)_6]\cdot yH_2O$ ($0\leqslant x\leqslant 1$, $1\leqslant y\leqslant 14$). Compounds within these two series were characterized from Infrared, Mössbauer, X-ray diffraction and thermo-gravimetric data, and magnetic measurements at low temperature. A model for their crystal structure is proposed and the structure for a representative composition refined from XRD powder patterns using the Rietveld method. A simple and reproducible procedure to prepare these solid solutions is provided. Within hexacyanoferrates, such mixed valence states system in both metal centres shows unique features, which are discussed from the obtained data.

Keywords: A. Magnetic materials; C. Mössbauer spectroscopy; D. Crystal structure; D. Magnetic properties; D. Electronic structure

1. Introduction

Prussian blue analogues have been extensively studied in the last decade due to their interesting magnetic properties, e.g. high T_c magnet [1–3], magnetic pole inversion [4], spin glass behaviour [5], magnetic refrigeration [6], and so on. Within Prussian blue analogues, cobalt hexacyanoferrates (II, III) have received a particular attention, mainly due to the observed photo-induced magnetism in cobalt (III) ferrocyanide [7,8]. The illumination of this compound induces an inner charge transfer to form cobalt (2+) ferricyanide, which shows magnetic order at low temperature (below 20 K). The heating of cobalt (2+) ferricyanide, above 353 K, induces the inverse charge transfer, to form low spin cobalt (III) ferrocyanide [9]. These two charge transfer processes indicate that in cobalt hexacyanoferrates (II,III) the energy barrier between high spin Co(2+) and low spin Co(III) is relatively low. Such behaviour for cobalt iron cyanide suggests the possibility of obtaining solid compounds with both Co and Fe in mixed valence sates as stable phase at room temperature. However, as far as we know, such possibility has not been explored. The preparation and study of materials based in these mixed valence states is the aim of this contribution. Two stable solid solutions of Co(2+)Co(III) hexacyanoferrates were prepared and characterized from X-ray diffraction (XRD), infrared (IR), Mössbauer, thermogravimetry and magnetic data. A structural model is proposed for these solid solutions and the crystal structure refined for a typical composition from XRD powder patterns using the Rietveld method. The crystal structures of related cobalt iron cyanides are provided as Supplementary Information.

*Corresponding author. Institute of Materials Science and Technology, University of Havana, 10400 Havana, Cuba. Tel./fax: 53 7 2096653.
E-mail address: ereguera@yahoo.com (E. Reguera).
[1]COFAA Fellow.

0022-3697/$ - see front matter © 2006 Elsevier Ltd. All rights reserved.
doi:10.1016/j.jpcs.2006.11.008

2. Experimental

2.1. Samples preparation

The samples of the mixed valence system to be studied were prepared with the following compositions: $(Co^{2+})_x(Co^{III})_{1-x}K[(Fe^{II})_{1-x}(Fe^{III})_x(CN)_6]\cdot\frac{1}{2}H_2O$ (MVS1 series), and $(Co^{2+})_{1.5x}(Co^{III})_{1-x}K[Fe^{II}(CN)_6]\cdot yH_2O$ (MVS2 series), with $0\leqslant x\leqslant 1$, $1\leqslant y\leqslant 14$. These compounds are obtained preparing an aqueous solution of appropriate molar mixtures of $K_3[Fe^{III}(CN)_6]$ and $K_4[Fe^{II}(CN)_6]$ and it then added under stirring to a solution of Co(2+) at room temperature. The formed precipitate was aged within the mother liquor for 24 h. The obtained solid is isolated by filtration, washed several times with distilled water and then air dried up to constant weight. MVS2 series compounds are obtained from equimolar mixtures of these soluble complex K salts, or using excess of the ferrous species. The MVS1 family is prepared from an excess of K ferricyanide (around 2:1 molar ratio or slightly smaller).

As will be discussed below, Co(2+) ferricyanide, $Co_3^{2+}[Fe^{III}(CN)_6]_2\cdot 14H_2O$, and the mixed salts, $Co^{2+}K_2[Fe^{II}(CN)_6]\cdot 2H_2O$ and $Co^{2+}Cs_2[Fe^{II}(CN)_6]$, in the following labelled as Co_3Fe_2, CoK_2Fe and $CoCs_2Fe$, respectively, are cobalt iron cyanides species closely related to the studied mixed valence compounds. Co_3Fe_2 (free of alkaline metal impurities) was obtained mixing aqueous solutions of Co(2+) sulphate and of ferricyanic acid ($H_3[Fe^{III}(CN)_6]$ prepared in situ [10]) under stirring, in a 3:2 molar ratio and then the precipitated solid separated, washed and dried as indicated above. The same procedure was used to obtain CoK_2Fe, but from potassium ferrocyanide. When the precipitation process from K ferrocyanide is carried out in the presence of Cs^+, or CoK_2Fe is boiled in an aqueous solution containing Cs^+ (ionic exchange), $CoCs_2Fe$ is obtained. These three compositions (Co_3Fe_2, CoK_2Fe and $CoCs_2Fe$) were used as reference compounds for the mixed valence system discussed in this contribution. Their refined crystal structures are available as Supplementary Information.

The nature of the studied samples as hexacyanoferrates was established through IR spectroscopy and their stoichiometry from the atomic ratio of the involved metals, derived from X-ray dispersed-energy spectra (EDS). The hydration degree was estimated from thermo-gravimetric (TG) curves. All the used reagents were analytical grade from Sigma-Aldrich.

2.2. Samples characterization

All the studied samples were characterized from XRD, IR, TG, Mössbauer and magnetic data. For Co_3Fe_2 and MVS2 series, which have a porous framework, also H_2O and N_2 adsorption isotherms were recorded.

IR spectra were collected by means of a Vector 22 spectrophotometer (Bruker). The IR spectra were recorded in Nujol mulls in order to avoid a mechano-chemical reaction of the sample with the alkali halide matrix. Hexacyanoferrates (III) react with alkali halides during the milling and disk preparation processes for IR spectroscopy [11]. Mössbauer spectra were run at 77 and 300 K with a constant acceleration spectrometer (from Wissel) operated in the transmission mode and a $^{57}Co/Rh$ source. The obtained spectra were fitted using a least-square minimization algorithm and pseudo-Lorentzian line shape in order to obtain the values for isomer shift (δ), quadrupole splitting (Δ), linewidth (Γ), and relative area (A). The values of δ are reported relative to sodium nitroprusside. The magnetic measurements were done at low temperature using a SQUID magnetometer (Quantum Design MPMS-XL7). The TGA curves were recorded under nitrogen flow in the Hi-Res mode of a TG-2950 thermo-balance (from TA Instruments) at a heating rate of 5 °C/min. XRD powder patterns were recorded in Bragg–Brentano geometry using a D8 Advance diffractometer (from Bruker) and monochromatic CuK_α radiation. Some XRD patterns were also recorded at the X10B-XPD beamline of the LNLS synchrotron radiation facilities (at Campinas, Brazil). *DicVol* program [12] was used to assign Miller indexes to the XRD powder patterns. The structural refinements were carried out with the *FullProf'2000* code [13] using pseudo-Voigt peak shape functions. Peak profiles were calculated within ten times the half linewidth. The background was modelled through a third order polynomial fitting.

N_2 adsorption isotherms were collected at 77 K using Accelerated Surface Area and Porosimetry system (ASAP 2010 model from Micromeritic). Water vapour adsorption isotherms were recorded at 303 K in home made equipment in which water is provided by evaporation from a calibrated capillar and the pressure measured by an oil manometer.

3. Results and discussion

3.1. Nature of the studied solids

In the case of Co_3Fe_2, CoK_2Fe and $CoCs_2Fe$ compounds, the atomic ratios Co:Fe, Co:K:Fe and Co:Cs:Fe, derived from EDS spectra, correspond approximately to the nominal compositions, 3:2, 1:2:1 and 1:2:1, respectively. However, for solids prepared from mixtures of potassium ferro- and ferri-cyanides (MVS1 and MVS2 series) a relatively wide range of stoichiometries, as elemental ratios of the involved metals, were obtained. Certain dependence of these elemental ratios on the used molar ratio of ferro- to ferri-cyanide was observed. This was interpreted as a probable formation of mixed valence compounds, in the sense here discussed, which was then confirmed from the IR, Mössbauer and magnetic data (discussed below).

MVS compounds, Co_3Fe_2, CoK_2Fe and $CoCs_2Fe$ can be distinguished by their colour. MVS series have a deep blue colour; similar to Prussian blues (class II mixed valence compounds [14]). Co_3Fe_2 is violet while CoK_2Fe and $CoCs_2Fe$ are grey.

Thermo-gravimetric analysis provided information on the hydration degree of the studied samples and also on the nature of the crystal water. Fig. 1 shows typical TG curves. On heating, Co_3Fe_2 becomes anhydrous below 100 °C preserving their crystal framework. Such behaviour is typical of zeolitic and weakly bonded water molecules. The amount of weight loss on dehydration process corresponds to the hydration degree indicated in the formula unit ($Co_3^{2+}[Fe^{III}(CN)_6]_2 \cdot 14H_2O$). Those compositions containing K, dehydrate at relatively higher temperature, suggesting that at least a fraction of the crystal water remains coordinated to the alkaline ion. $CoCs_2Fe$ was found to be anhydrous. However, for MVS compositions, particularly for MVS2 series, a mixed behaviour was observed, with a partial dehydration similar to that found for Co_3Fe_2 and then at a higher temperature, those water molecules sited in the coordination environment of the K^+ ion evolve. Once dehydrated, these compounds remain stable up to above 250 °C, except Co_3Fe_2 and those compositions corresponding to the MVS1 series, where a heat-induced charge transfer takes place [9]. Above 250 °C a progressive partial decomposition of the sample is observed, releasing CN^- ligands. The liberated CN^- groups reduce the involved metals and C_2N_2 as gaseous species evolves [15]. In MVS compounds the reduction of Co(3+) to Co(2+) could also take place.

IR spectra of hexacyanometallates are composed of three absorption bands related to vibrations within the octahedral unit $Fe(CN)_6$, ν(CN), δ(FeCN) and ν(FeC) and those from crystallization water, ν(OH) and δ(HOH) [16]. Table 1 collects the frequency of these vibrations for the studied samples. The ν(CN) band frequency is a sensor of the triple bond strength and of the nature of the chains that are forming the framework and it allows an unequivocal differentiation between ferro- and ferri-cyanides [17].

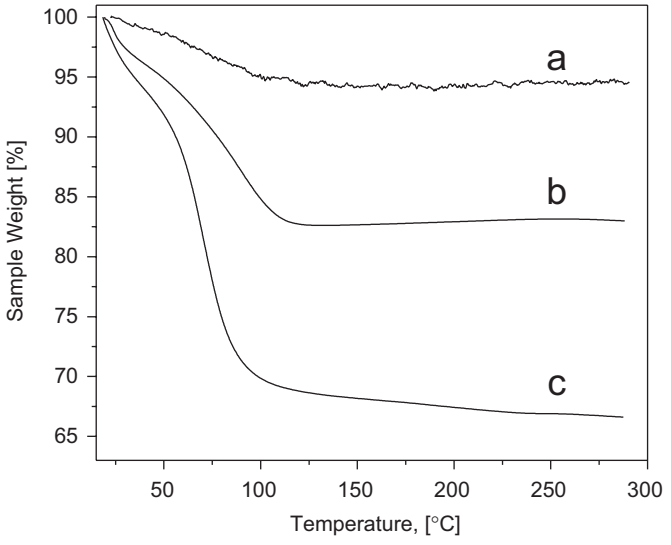

Fig. 1. Thermo-gravimetric curves of: (a) $(Co^{2+})_{1.5x}(Co^{III})_{1-x}K[Fe^{II}(CN)_6] \cdot yH_2O$, (b) $Co^{2+}K_2[Fe^{II}(CN)_6] \cdot 2H_2O$ and (c) $Co_3^{2+}[Fe^{III}(CN)_6]_2 \cdot 14H_2O$.

Table 1
Observed IR frequencies (cm^{-1}) for the studied cobalt iron cyanide samples

Sample	ν(CN)	δ(FeCN)	ν(FeC)	ν(OH)	δ(HOH)
$CoCs_2Fe$	2080	591	460	—	—
CoK_2Fe	2080	591	455	3362 (Broad)	1610
Co_3Fe_2	2160(s) 2120(w) 2080(w)	544	432	3407 (Broad)	1609
MVS1	2160, 2120–2080	591–544	460–432	3388 (Broad)	1610
MVS2	2120–2080	591–560	460–450	3388 (Broad)	1610

s: strong.
w: weak.

Ferricyanides usually have this vibration 80 cm^{-1} above ferrocyanides. The frequency of the ν(CN) vibration is determined by the valence of both, the inner and the outer metal, and by the intensity of the π back-bonding interaction between the iron atom and the CN ligands. This interaction is stronger in ferrocyanides because low spin Fe(II) has a higher availability of electrons in its t_{2g} orbitals. An increase in the metal t_{2g} electron delocalization on the π^* orbitals of the CN ligand leads to a weakening in its triple bond. This brings about a decrease in the frequency of the ν(CN) vibration. For cobalt (2+) ferricyanide this band is observed at 2160 cm^{-1} while for mixed ferrocyanides, CoK_2Fe and $CoCs_2Fe$, it is found at 2080 cm^{-1} (Fig. 2). However, for MVS compounds, a band of intermediate frequency, between 2130 and 2080 cm^{-1}, appears (Fig. 2). The presence of this band suggests the oxidation of high spin Co(2+) to low spin Co(III), involving the change of electronic configuration. In the low spin state the e_g orbitals of Co(III) are free to receive electrons from the CN ligands, mainly from their 5σ orbitals which are weakly antibonding. This strengthens the CN bond and increases the ν(CN) vibration frequency, relative to Co(2+) ferrocyanide. The oxidation of Co(2+) to Co(3+) during the MVS complexes preparation could take place at expense of the potassium ferricyanide reduction, at least of a fraction of this last one, during the solid precipitation. Such redox process could also be present during the preparation of Co_3Fe_2 since in its IR spectra weak ν(CN) bands at 2120 and 2080 cm^{-1} are always observed (Fig. 2a), but at relatively low concentration because in the XRD powder pattern of Co_3Fe_2 samples only reflection of pure cobalt(2+) ferricyanide appear (discussed below).

From a structural point of view, the existence of only one ν(CN) absorption band in CoK_2Fe and $CoCs_2Fe$ at 2080 cm^{-1} reveals the presence of only one type of chain in their framework, Fe^{II}–C≡N–Co^{2+}. For MVS compounds, up to three ν(CN) absorption bands are observed, corresponding to Fe^{III}–C≡N–Co^{2+}, Fe^{II}–C≡N–Co^{III} and Fe^{II}–C≡N–Co^{2+} chains (Fig. 2). Those compositions containing these three ν(CN) absorptions were labelled MVS1. With the label MVS2 those MVS species with

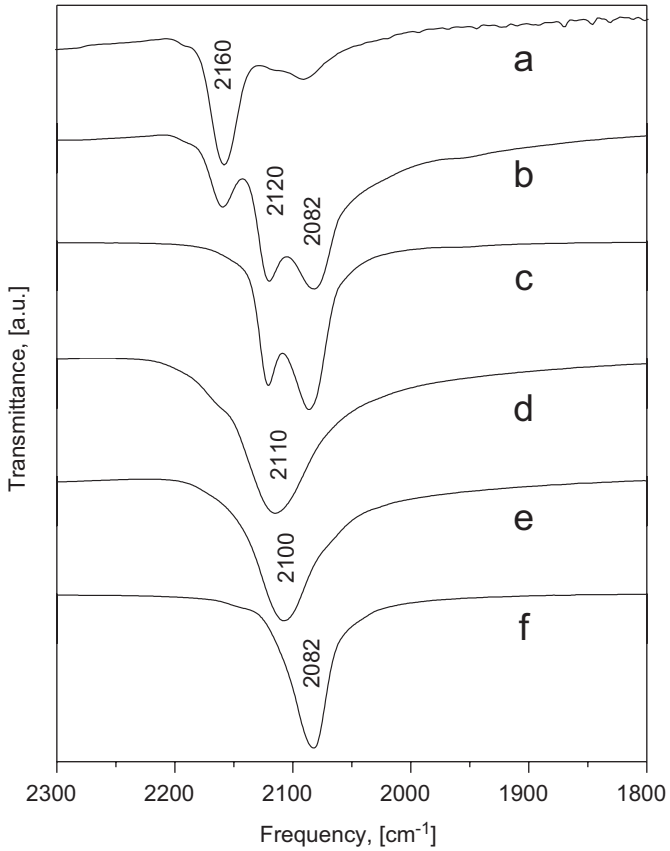

Fig. 2. IR spectra (ν(CN) vibration region) of: a) $Co_3^{2+}[Fe^{III}(CN)_6]_2 \cdot 14H_2O$, (b) $(Co^{2+})_x(Co^{III})_{1-x}K[(Fe^{II})_{1-x}(Fe^{III})_x(CN)_6] \cdot \frac{1}{2}H_2O$, (c, d) $(Co^{2+})_{1.5x}(Co^{3+})_{1-x}K[Fe^{II}(CN)_6] \cdot yH_2O$, (e) $Co^{2+}K_2[Fe^{II}(CN)_6] \cdot 2H_2O$.

absence of the ferric contribution (Fe^{III}–C≡N–Co^{2+}) are designed. The framework of these mixed valence compounds both MVS1 and MVS2 series, could be formed as a random mixture of the corresponding structural chains, where the proportion of the involved chains would be determined by the molar ratio used during the sample preparation.

The XRD powder patterns obtained for the MVS samples correspond to the $Pmn2_1$ space group (orthorhombic cell) found for CoK_2Fe (Fig. 3). In this space group also crystallize the Mn, Ni and Cd analogues (MnK_2Fe, NiK_2Fe, CdK_2Fe) [18,19]. For MVS1 series prepared with a large excess of potassium ferricyanide, a mixture of Co(2+) ferricyanide, with a cubic (Fm-3m) cell and of the orthorhombic ($Pmn2_1$) phase is obtained. However, for molar ratio around 2:1, only the orthorhombic phase results, with ν(CN) absorptions at 2160, 2120 and 2080 cm^{-1} (Fig. 2b). This indicates that the $Pmn2_1$ structure can be formed as mixture of Fe^{III}–C≡N–Co^{2+}, Fe^{II}–C≡N–Co^{III} and Fe^{II}–C≡N–Co^{2+} chains (MVS1 series).

The studied materials can be considered as a 3D assembling of practically rigid octahedral blocks, $Fe(CN)_6$, which remain bridged at their N ends through cobalt atoms, also in an octahedral coordination. This is a useful

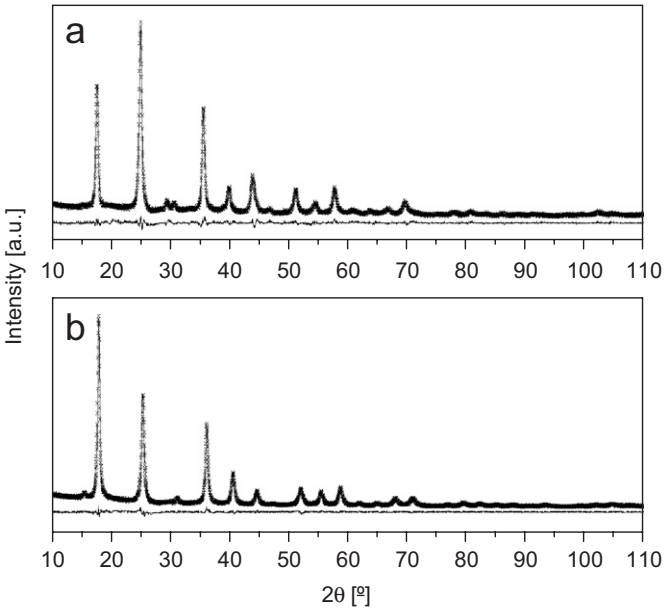

Fig. 3. Experimental and calculated XRD powder patterns, and their difference of: (a) $Co^{2+}K_2[Fe^{II}(CN)_6] \cdot H_2O$, (b) $(Co^{2+})_{0.57}(Co^{III})_{0.43}K[(Fe^{II})_{0.43}(Fe^{III})_{0.57}(CN)_6] \cdot H_2O$.

approximation to refine their crystal structure from XRD powder patterns using the Rietveld method. The C–N and Fe–C distances and the bond angles within the octahedral unit can be restricted to take values within certain given intervals with also restricted variation limits. The starting values of these parameters and the allowed variation limits can be taken from crystal structures of analogues compounds resolved using the single crystal method [20,21]. In such 3D arrangement of octahedral units, the alkali metal plays the role of charge balance cation sited in interstitial positions. In principle, these extra-framework metals are exchangeable species if the framework windows (and channels) allow their diffusion through the solid.

3.2. Crystal structure of $(Co^{2+})_x(Co^{III})_{1-x}K[(Fe^{II})_{1-x}(Fe^{III})_x(CN)_6] \cdot \frac{1}{2}H_2O$

As already mentioned, the studied MVS compounds were found to be isomorphous to CoK_2Fe, with an orthorhombic unit cell (space group $Pmn2_1$). Two formula units ($Z = 2$) are accommodated within the unit cell. This orthorhombic cell results from a local distortion of the cubic one (Fm-3m) mainly originated from hydrated potassium atoms sited in interstitial positions. During the crystallization process, the charge balance K^+ ion retains a fraction of its hydration water. The accommodation of this relatively large and asymmetric K-OH_2 unit within the small interstitial voids leads to certain local distortion of the neighbouring –C≡N– bridges, which changes the crystal symmetry. That local distortion also has certain contribution from structural units of different size, the octahedral blocks, $Fe^{II}(CN)_6$ and $Fe^{III}(CN)_6$), and the metal ions that join these blocks, high spin Co^{2+} and low

spin Co^{III}. The orthorhombic cell is closely related to the cubic (Fm-3m) one where $CoCs_2Fe$ and Co_3Fe_2 crystallize. In fact, one of its cell edges (**a**) corresponds to the Fe–C≡N–Co–N≡C–Fe chain length. In the cubic cell volume two orthorhombic cells could be accommodated.

The crystal structure to be refined corresponds to a MVS1 composition with $x = 0.57$ (estimated from Mössbauer spectroscopy results, discussed below), with cell edges: $\mathbf{a} = 9.933(2)$, $\mathbf{b} = 6.989(1)$, $\mathbf{c} = 7.066(1)$ Å. From the above description for the MVS compounds framework, the crystal structure of this composition was refined sitting the Fe and Co atoms in 2a positions, $(0, y, z)$ for iron and $(\frac{1}{2}, y, z)$ for cobalt; C and N ones in 4b (x, y, z) and 2a $(0, y, z)$ sites, and K and the O atom from water also sited in the general 4b (x, y, z) site. This corresponds to a compact structure with a unitary occupation factor for all the atoms, except for K and water which is $\frac{1}{2}$ and $\frac{1}{4}$, respectively. This model produced an excellent pattern fitting ($S = 1.45$) and good figures of merit for the refinement process ($R_{exp} = 5.05$; $R_p = 5.79$; $R_{wp} = 6.30$; $R_B = 5.42$). The refined atomic positions and thermal factors are reported in Table 2. The calculated bond distances and angles appear in Table 3. The obtained K–OH_2 distance falls within the reported values for hydrated potassium salts, e.g. $KF.4H_2O$ (K–O: 2.79(2) Å) [22].

The hydration degree for this MVS1 composition, derived from the TG curve is slightly higher, close to a water molecule per formula unit, probably due to existence of weakly bonded surface water, which has a minor effect on XRD powder pattern.

Compounds of MVS2 series can also be refined in that structural model resulting slightly different cell edges and bond distances and angles. However, this model and the resulting values for inter-atomic distances and bond angles in both series must be taken as average results, due to the nature of MVS compounds as solid solutions. Conclusive evidence in this sense is obtained from Mössbauer spectroscopy (discussed below).

MVS compounds show certain porosity, particularly those from MVS2 series, due to systematic vacancies of the octahedral block, $Fe(CN)_6$. This is appreciated in the corresponding water vapour adsorption isotherm (Fig. 4). In the limit case, without Co(III) ions, compounds of this series have a porosity similar to that observed for Co_3Fe_2, where up to 14 water molecules can be accommodated within a pore, six of them coordinated to cobalt atoms. The adsorption of N_2 also corresponds to a porous framework.

3.3. Mössbauer spectra

The CN group is a strong ligand at its C end forcing to a low spin electronic configuration for the metal coordinated

Table 3
Bond distances (in Å) and bond angles (in °) for $(Co^{2+})_{0.57}(Co^{III})_{0.43}K[(Fe^{II})_{0.43}(Fe^{III})_{0.57}(CN)_6]\cdot\frac{1}{2}H_2O$

	Bond	Distances
Fe–C1: 1.929(2)	C1–N1: 1.150(6)	Co–N1: 1.906(3)
Fe–C2: 1.928(3)	C2–N2: 1.151(11)	Co–N2: 2.081(24)
Fe–C3: 1.929(29)	C3–N3: 1.150(31)	Co–N3: 1.879(27)
Fe–C4: 1.929(6)	C4–N4: 1.151(29)	Co–N4: 1.896(23)
Fe–C5: 1.928(7)	C5–N5: 1.150(17)	Co–N5: 2.102(37)
		K–O: 2.699(31)
	Bond	Angles
C1–Fe–C1: 172.7(8)	Fe–C1–N1: 169.3(8)	N1–Co–N1: 174.4(6)
C1–Fe–C2: 92.1(9)	Fe–C2–N2: 142.0(18)	N1–Co–N2: 89.0(14)
C1–Fe–C3: 87.2(16)	Fe–C3–N3: 177.6(30)	N1–Co–N3: 90.8(18)
C1–Fe–C4: 87.1(9)	Fe–C4–N4: 162.5(22)	N1–Co–N4: 92.5(18)
C1–Fe–C5: 92.3(7)	Fe–C5–N5: 147.3(22)	N1–Co–N5: 92.5(15)

Table 2
Refined atomic positions for $(Co^{2+})_{0.57}(Co^{III})_{0.43}K[(Fe^{II})_{0.43}(Fe^{III})_{0.57}(CN)_6]\cdot\frac{1}{2}H_2O$

	Site	x	y	z	Biso	Occ
Fe	2a	0	0.2413(2)	−0.0069(2)	1.2(3)	1
Co	2a	0.5	0.2581(4)	−0.0006(2)	0.5(2)	1
C1	4b	0.1938(2)	0.2418(33)	−0.0243(7)	0.54(11)	1
C2	2a	0	0.0120(2)	0.1448(4)	0.54(11)	1
C3	2a	0	0.4208(43)	−0.2142(4)	0.54(11)	1
C4	2a	0	0.0793(9)	−0.2279(9)	0.54(11)	1
C5	2a	0	0.4494(6)	0.1723(2)	0.54(11)	1
N1	4b	0.3083(2)	0.2631(29)	−0.0128(9)	0.54(11)	1
N2	2a	0	−0.0396(7)	0.2994(12)	0.54(11)	1
N3	2a	0	0.5331(37)	−0.3332(3)	0.54(11)	1
N4	2a	0	−0.0530(3)	−0.3250(2)	0.54(11)	1
N5	2a	0	0.4956(47)	0.3285(13)	0.54(11)	1
K	4b	−0.2737(6)	−0.2772(7)	−0.0284(5)	4.28(22)	$\frac{1}{2}$
O	4b	−0.010(5)	−0.1953(8)	−0.066(6)	9(1)	$\frac{1}{4}$

Number of observations: 4001; Number of reflections: 730; Number of distance constrained: 3 (Fe–C, C–N and K–O).

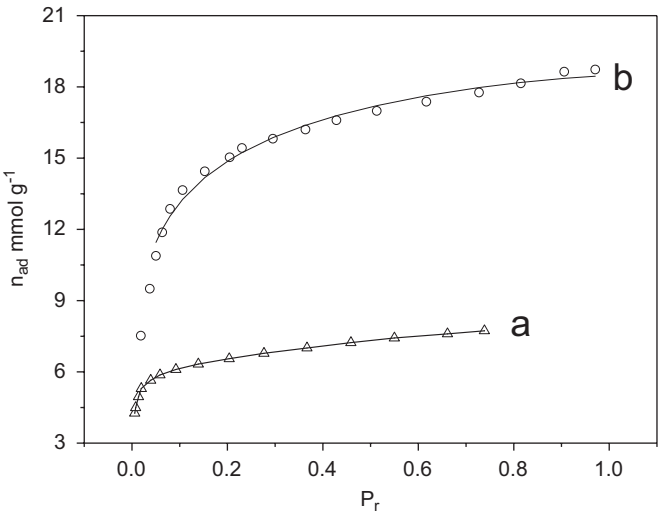

Fig. 4. Water vapour adsorption isotherms in: (a) $(Co^{2+})_{1.5x}(Co^{III})_{1-x}K[Fe^{II}(CN)_6]$, (b) $Co_3^{2+}[Fe^{III}(CN)_6]_2$.

Table 4
Mössbauer parameters at room temperature and 77 K for the studied cobalt iron cyanide samples

Sample	Temp (K)	δ[a] (mm/s)	Δ (mm/s)	Γ (mm/s)	A (%)	Assign
$CoCs_2Fe$	300	0.16	—	0.36	100	LS Fe(II)
$CoCs_2Fe$	77	0.24	—	0.52	100	LS Fe(II)
CoK_2Fe	300	0.17	—	0.31	100	LS Fe(II)
CoK_2Fe	77	0.25	—	0.42	100	LS Fe(II)
Co_3Fe_2	300	0.11	0.42	0.35	100	LS Fe(III)
Co_3Fe_2	77	0.19	0.85	0.46	100	LS Fe(III)
MVS1	300	0.11	0.42	0.31	57	LS Fe(III)
		0.16	0.66	0.30	24	LS Fe(II)
		0.15	0.30	0.29	19	LS Fe(II)
MVS1	77	0.19	0.80	0.49	56	LS Fe(III)
		0.24	0.58	0.40	23	LS Fe(II)
		0.25	0.28	0.35	21	LS Fe(II)
MVS2	300	0.16	0.64	0.25	57	LS Fe(II)
		0.16	0.27	0.34	43	LS Fe(II)
MVS2	77	0.24	0.63	0.48	55	LS Fe(II)
		0.23	0.24	0.32	45	LS Fe(II)

[a] δ values are reported relative to sodium nitroprusside.

by the C atom side. From this fact, in hexacyanoferrates the iron atom is always found in low spin state. At the same time, the CN ligand has a low energy π-anti-bonding orbital at its C end which abstracts electron from $d_{x,y}$, $d_{x,z}$, and $d_{y,z}$ orbitals of the inner metal.

This π-back bonding interaction leads to a significant reduction of the 3d electron shielding effect on the s-electron density at the iron nucleus, explaining the extremely low values of isomer shift (δ) in hexacyanoferrates (Table 4). As expected, Mössbauer spectra of CoK_2Fe and $CoCs_2Fe$ are single lines (Figs. 5, 6) related to the high symmetry for the iron atom environment, and also to the symmetry of its filled t_{2g} orbitals. Mössbauer spectrum of Co_3Fe_2 is a quadrupole doublet, mainly due to the unpaired electron in the iron t_{2g} orbitals but, probably also due to certain contribution from an asymmetrical π-back bonding interaction, originated by the Co atoms at the pore surface. When the spectrum of Co_3Fe_2 is taken at 77 K (Fig. 6) the first contribution to Δ (quadrupole splitting) is enhanced, because on cooling the electronic distribution of low spin iron(III) becomes more asymmetric, producing a higher value of Δ. Mössbauer spectra of MVS1 series usually appear as three quadrupole doublets, one of them from low spin Fe(III) and the other two ones from low spin Fe(II) (Table 4). A conclusive evidence for this assignment is obtained comparing spectra recorded at 300 and 77 K. Only for one of these three doublets the value of Δ appears temperature sensitive (Figs. 5, 6) indicating that it proceeds from low spin Fe(III). The other two doublets, of smaller quadrupole splitting values (Δ), result from a cell contribution to the electric field gradient around the iron nucleus. For compounds of MVS2 series, Mössbauer spectra only show doublets of low spin Fe(II) (temperature insensitive). Samples obtained from 1:1 molar ratio or with a slight

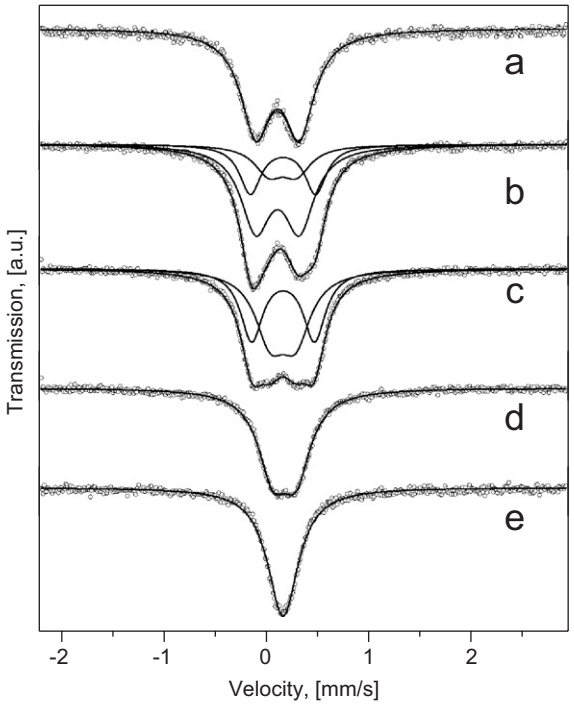

Fig. 5. Mössbauer spectra at room temperature of: (a) $Co_3^{2+}[Fe^{III}(CN)_6]_2 \cdot 14H_2O$; (b) $(Co^{2+})_x(Co^{III})_{1-x}K[(Fe^{II})_{1-x}(Fe^{III})_x(CN)_6] \cdot \frac{1}{2}H_2O$ (MVS1); (c, d) $(Co^{2+})_{1.5x}(Co^{III})_{1-x}K[Fe^{II}(CN)_6] \cdot yH_2O$ (MVS2); (e) $Co^{2+}K_2[Fe^{II}(CN)_6] \cdot H_2O$.

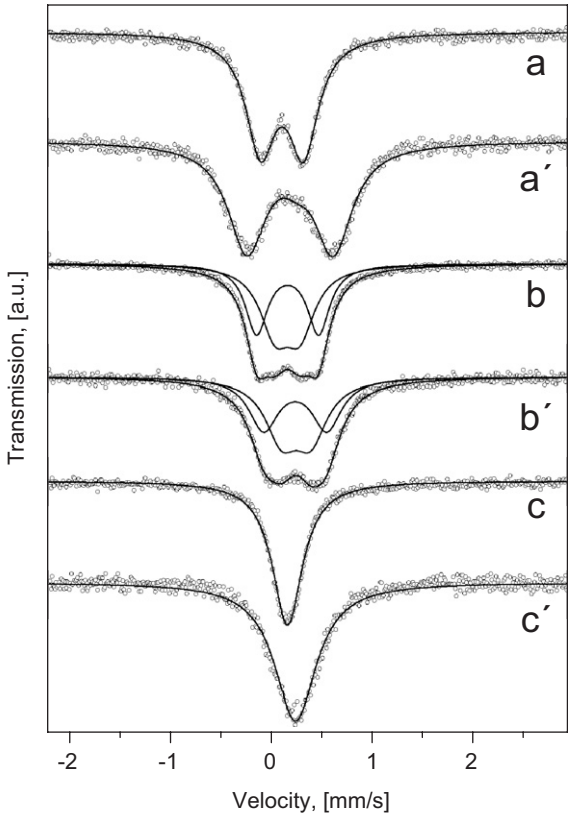

Fig. 6. Mössbauer spectra of: $Co_3[Fe^{III}(CN)_6]_2 \cdot 14H_2O$ at room temperature (RT) (a) and at 77 K (a′); $(Co^{2+})_{1.5x}(Co^{III})_{1-x}K[Fe^{II}(CN)_6] \cdot yH_2O$ (MVS2) at RT (b) and at 77 K (b′); $Co^{2+}K_2[Fe^{II}(CN)_6] \cdot H_2O$ at RT (c) and at 77 K (c′).

excess of K ferrocyanide show two of such doublets. A higher concentration of this last K salt leads to a decrease in the intensity of one of these two doublets which disappears from mixtures about 1:3 molar ratio. In this case the resulting Mössbauer spectra only show a doublet with a relatively small value of Δ (Fig. 5d). Probably this small value of Δ for MVS2 compositions rich in Co^{2+}–N ≡ C–Fe^{II} species, is related to the existence of vacancies of the $Fe(CN)_6$ building unit. The resulting large pores could help to "absorb" the local distortions around the iron atoms, which is sensed through a low Δ value. In the limit case, of a very low population of Co(III) ions, the resulting Mössbauer spectra must be a single line, with an isomer shift (δ) value similar to that obtained for CoK_2Fe and $CoCs_2Fe$ (Table 4).

Only a small difference, of about 0.05 mm/s, is observed between isomer shift values of ferrous and ferric species (Table 4). The higher availability of t_{2g} electrons in low spin Fe(II) favours a more pronounced π-back donation towards the CN ligands in this ion and the net effect is an iron atom with a t_{2g} population of electrons practically similar to that found in low spin Fe(III). However, that small difference helps to differentiate between ferric and ferrous species in the studied materials, particularly for compounds of the MVS1 series (Fig. 5b, Table 4). The observed increase in the value of δ on cooling results from a temperature effect (second order Doppler shift) and not to changes in the electronic structure of the studied samples.

The calculated values of relative area of sub-spectrum derived from Mössbauer spectra fitting, allow an estimation of the relative population of iron(III) and iron(II) atoms in different structural sites. For instance, from 1:1 molar ratio of K ferri- and ferro-cyanide, the resulting solid is free of ferric species, with two different sites for the iron atom of similar relative populations. The refined crystal structure corresponds to a sample with 57% of Fe(III), according to the estimated relative area of ferric signal. This procedure to estimate the relative population of iron atoms in a given site supposes that all the sites have equal value for the Mössbauer absorption probability. This could be an acceptable hypothesis because all of them belong to a same framework with similar ligands.

3.4. Magnetic measurements

According to the magnetization curves versus temperature for $CoCs_2Fe$ and CoK_2Fe, these compositions show non-magnetic order, at least at 4 K, an obvious result from the obtained Mössbauer spectroscopy information. The iron atoms are in a low spin electronic configuration ($S = 0$) and the Co ones ($S = \frac{3}{2}$) remain separated by approximately 10 Å, probably with a weak anti-ferromagnetic interaction.

Co_3Fe_2 and compounds from MVS1 series show a definite magnetic order below 20 K, related to the existence of Fe^{III}–C≡N–Co^{2+}–N≡C–Fe^{III} chains in their framework. In the mass susceptibility per temperature versus temperature, $\chi_p T$ versus T, curves a maximum around certain critical temperature (Curie temperature, T_c) appears (Fig. 7). Such behaviour indicates the existence of ferrimagnetic order in these compounds, which results from a combined effect of both a ferromagnetic interaction due to overlapping of orthogonal e_g and t_{2g} orbitals from Co^{2+} and Fe^{III} atoms, respectively, and from an antiferromagnetic interaction between t_{2g} orbitals from Co^{2+} and Fe^{III}. These compounds contain chains with unpaired spins on the metal centres and the CN ligand allows a strong overlapping of their electron clouds facilitating the occurrence of magnetic order. For Co_3Fe_2 the estimated value of T_c is 13 K, similar to that already reported for this composition [9,23] while for a MVS1 composition with 57% of ferric species (Fig. 5b) T_c results to be close to 11 K. In the following, all the reported magnetic data for MVS compounds correspond to that composition (57% of ferric species). As lesser is the ferric fraction, lower is the T_c value and, in the limit case (MVS2 series), no magnetic order is observed (Fig. 7).

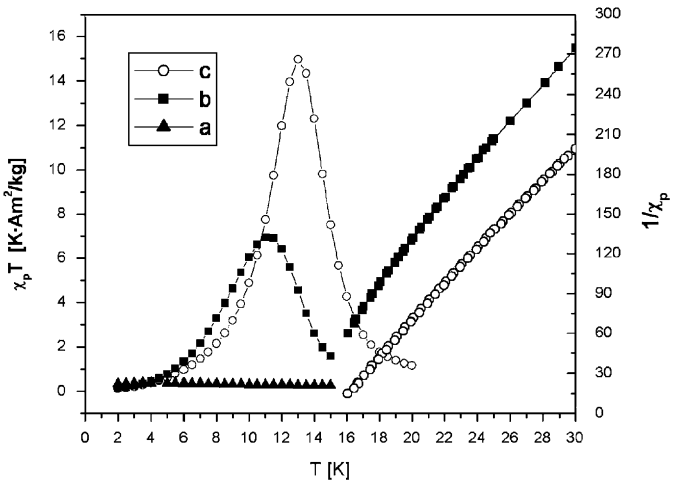

Fig. 7. Massic magnetic susceptibility per temperature ($\chi_p T$) versus temperature (T) for: (a) $(Co^{2+})_{1.5x}(Co^{III})_{1-x}K[Fe^{II}(CN)_6]\cdot yH_2O$ (MVS2); (b) $(Co^{2+})_x(Co^{III})_{1-x}K[(Fe^{II})_{1-x}(Fe^{III})_x(CN)_6]\cdot\frac{1}{2}H_2O$ (MVS1); (c) $Co_3^{2+}[Fe^{III}(CN)_6]_2\cdot 14H_2O$. Included also are the ($1/\chi_p$) versus T dependence (right curves) used to estimate the Curie temperature, T_c.

The isothermal magnetization curves of Co_3Fe_2 and $(Co^{2+})_{0.57}(Co^{III})_{0.43}K[(Fe^{II})_{0.43}(Fe^{III})_{0.57}(CN)_6]\cdot\frac{1}{2}H_2O$ at 4 K show hysteresis loops characteristic of magnetic materials (Fig. 8). For Co_3Fe_2, the values of remanence and coercive field, 14 Am^2/kg and 197.4 kA/m, respectively, similar to those previously reported [9,23]. The studied MVS1 composition has a residual magnetization of 8 Am^2/kg, which represents 57% of the value obtained for Co_3Fe_2. This can be attributed to the existence of certain amount of non-magnetic chains (Co(III)($S = 0$)–NC–Fe(II)($S = 0$)) within the structure of this material. The coercive field is also lesser for this compound, 136.9 kA/m, 66% of the observed value for Co_3Fe_2. The saturation magnetization follows the same behaviour, 43 and 38 Am^2/kg, for Co_3Fe_2 and the MVS1 complex, respectively. Co_3Fe_2 has a porous

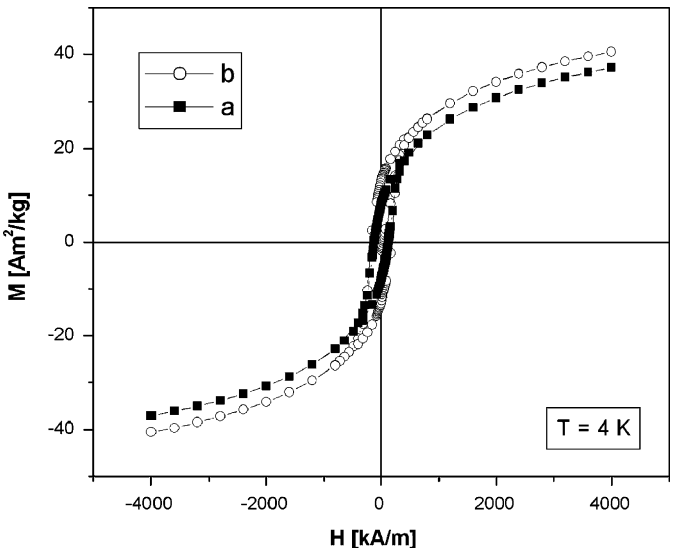

Fig. 8. Hysteresis loops at 4 K for: (a) $(Co^{2+})_{0.57}(Co^{III})_{0.43}K[(Fe^{II})_{0.43}(Fe^{III})_{0.57}(CN)_6]\cdot\frac{1}{2}H_2O$, (b) $Co_3^{2+}[Fe^{III}(CN)_6]_2\cdot 14H_2O$.

structure that is an unfavourable factor for a strong magnetic interaction, while the other composition has a compact structure but with some non-magnetic chains. From these facts, the obtained values for parameters related to their magnetic properties only allow a qualitative comparison.

Fig. 7 shows the temperature dependence of the reciprocal of the measured mass susceptibility (χ_p), for both $(Co^{2+})_{0.57}(Co^{III})_{0.43}K[(Fe^{II})_{0.43}(Fe^{III})_{0.57}(CN)_6]\cdot\frac{1}{2}H_2O$ and Co_3Fe_2 (for comparison), which behaves as a straight line down to 17 K, where a small inflection appears. That inflection was interpreted as appearance of certain anti-ferromagnetic interaction, with an estimated Néel temperature ($T_{Néel}$) of 15.4 and 13.9 K, respectively. Extrapolating the linear region of these dependences up to the x-axis, the Curie–Weiss temperature (θ_{CW}) was estimated, resulting 14 and 12 K, for Co_3Fe_2 and the MVS1 compound, respectively. These positive values of θ_{CW} are in correspondence with the existence of a net ferrimagnetic coupling in these compounds. The Curie constant, C, and a more precise values for θ_{CW} were obtained from a fitting of the experimental data according to the Curie–Weiss law: $\chi^{-1} = (T-\theta_{CW})/C$. The C values from that linear fitting are: 0.09 and 0.06 K, for Co_3Fe_2 and MVS1 sample, respectively; while θ_{CW} results in: 11.8 K (Co_3Fe_2) and 11.6 K (MVS1).

The effective magnetic moment, p_m, was estimated from the derived values for the Curie constant, according to: $C = N_A\mu_B\rho p_m^2/3k_BM'$, where ρ is the material density (estimated from the refined crystal structures), k_B is the Bolztmann constant, N_A the Avogadro's number, and M′ is the molecular weight. The resulting values for p_m were $6.7\mu_B$ for Co_3Fe_2 and $3.2\mu_B$ in the MVS1 complex.

The above-discussed magnetic data help to support the nature of the studied MVS system as solid solutions of high spin Co(2+) low spin Co(III) hexacyanoferrates (III,II) for MVS1 series and as high spin Co(2+) low spin Co(III) hexacyanoferrates (II) for MVS2 series.

Analogues MVS of Co(2+)Co(III) hexacyanoferrates have been found from a heat-induced charge transfer in Co(2+) hexacyanoferrate (III) [9]. However, in that case the resulting solid solution preserves the Fm-3m structure of the parent compound, with only a progressive cell contraction which senses the charge transfer process. Such behaviour was not observed for the MVS system reported in this contribution where two series of solid solutions, non-cubic, were found.

Mixed valence states in the two metal centres have been reported for manganese hexacyanoferrates [24]. However, using the procedure above discussed to obtain the MVS compounds here studied, always a mixture of Mn(2+) hexacyanoferrate (III) and of Mn(2+) hexacyanoferrate (II), as independent phases, was obtained.

4. Conclusions

In addition to Co(2+) hexacyanoferrates (II,III), in the cobalt iron cyanide system also mixed valence states involving high spin Co(2+) and low spin Co(III) species, as stable phases, can be formed. To the Co^{III}–NC–Fe^{II} chain corresponds an intermediate ν(CN) absorption in IR spectra which falls around 2120 cm^{-1}, 40 cm^{-1} below and above the frequency values of this vibration in Co(2+) ferri- and ferro-cyanides, respectively. In samples prepared from mixtures of K ferri- and ferro-cyanides, Fe^{III}–C≡N–Co^{2+}, Fe^{II}–C≡N–Co^{III} and Fe^{II}–C≡N–Co^{2+} species can be present within a same framework as a single phase and in different proportions, which corresponds to the following formula unit: $(Co^{2+})_x(Co^{III})_{1-x}K[(Fe^{II})_{1-x}(Fe^{III})_x(CN)_6]\cdot\frac{1}{2}H_2O$ ($0\leqslant x\leqslant 1$). Such MVS compounds form a true solid solution. This series of MVS complexes shows magnetic order at low temperature with a T_c value that decreases as does the amount of ferric species in the sample. For this series Mössbauer spectra reveal the existence of low spin Fe(III) (one structural site) and low spin Fe(II), this last one in two non-equivalent structural sites. This assignment was confirmed comparing Mössbauer spectra recorded at 300 and at 77 K. MVS compounds, free of ferric species, are also possible, forming a solid solution with the following formula unit: $(Co^{2+})_{1.5x}(Co^{III})_{1-x}K[Fe^{II}(CN)_6]\cdot yH_2O$ ($0\leqslant x\leqslant 1$, $1\leqslant y\leqslant 14$). No magnetic order was observed for this series and the corresponding Mössbauer spectra are quadrupole doublets due to certain lattice contribution to the electric field gradient around the iron atoms. This was interpreted as resulting from the slightly different ionic radii for high spin Co(2+) and low spin Co(III), and also from certain local distortion induced by mono-hydrated K^+ sited in interstitial positions. All the studied MVS compounds were found to be orthorhombic (space group $Pmn2_1$). A structural model was proposed for these families of

compounds and the crystal structure refined for a representative composition.

Acknowledgments

The authors thank LNLS synchrotron radiation facility (at Campinas, Brazil) for the acquisition of XRD data through the research Grant 3275-2005. R.M.G thanks the support provided by the CLAF-ICTP program for his PhD studies. E.R. acknowledges the support received from CLAF-ICTP to carry out research activities on molecular materials. Support from CNPq and FAPESP (Brazilian agencies) is also acknowledged.

Appendix A. Supplementary material

Supplementary data associated with this article can be found in the online version at doi:10.1016/j.jpcs.2006.11.008.

References

[1] S. Ferlay, T. Mallah, R. Ouahes, P. Veillet, M. Verdaguer, Nature 378 (1995) 701.
[2] S.M. Holmes, G.S. Girolami, J. Am. Chem. Soc. 121 (1999) 5593.
[3] M. Verdaguer, A. Bleuzen, V. Marvaud, J. Vaissermann, M. Seuleiman, C. Desplanches, A. Scuiller, C. Train, R. Garde, G. Gelly, C. Lomenech, I. Rosenman, P. Veillet, C. Cartier, F. Villain, Coord. Chem. Rev. 192 (1999) 1023.
[4] S. Ohkoshi, K. Arai, Y. Sato, K. Hashimoto, Nature Mater 3 (2004) 857.
[5] W.E. Buschmann, J. Ensling, P. Gütlich, J.S. Miller, Chem. Eur. J. 5 (1999) 3019.
[6] E. Manuel, M. Evangelisti, M. Affronte, M. Okubo, C. Train, M. Verdaguer, Phys. Rev. B 73 (2006) 172406.
[7] O. Sato, T. Iyoda, A. Fujishima, K. Hashimoto, Science 272 (1996) 704.
[8] O. Sato, Acc. Chem. Res. 36 (2003) 692 and references therein.
[9] R. Martínez-García, M. Knobel, E. Reguera, J. Phys. B 110 (2006) 7296.
[10] G. Brauer, Handbook of Preparative Inorganic Chemsitry, second ed., vol. 2, Academic Press, New York, 1965, p. 1373
[11] J. Fernandez, E. Reguera, Solid State Ionics 93 (1997) 139.
[12] D. Louer, R. Vargas, J. Appl. Cryst. 15 (1982) 542.
[13] J. Rodriguez-Carbajal, The FULLPROF Program, Institute Leon Brillouin, Saclay, France 2000.
[14] P. Day, A. Ludi, in: D.B. Brown (Eds.), Mixed-Valance Compounds; Theory and Application in Chemistry, Physics, Geology and Biology, NATO Advanced Study Institute Series C, vol. 58, pp. 3–24, 25–47, Reidel, Dordrecht, 1980.
[15] E. Reguera, J. Balmaseda, G. Quintana, J. Fernández, Polyhedron 17 (1998) 2353.
[16] E. Manuel, M. Evangelisti, M. Affronte, M. Okubo, C. Train, M. Verdaguer, Phys. Rev. B 73 (2006) 172406.
[17] E. Reguera, J. Fernandez, J. Balmaseda, Transition. Met. Chem. 24 (1999) 648.
[18] R. Martinez-Garcia, E. Reguera, J. Balmaceda, G. Ramos, H. Yee-Madeira, Powder Diffract. 19 (2004) 285.
[19] R. Martinez-Garcia, E. Reguera, J. Rodríguez, J. Balmaseda, J. Roque, Powder Diffract. 19 (2004) 255.
[20] G. Beall, W. Milligan, J. Korp, I. Bernal, Inorg. Chem. 16 (1977) 2715.
[21] F. Herren, P. Fischer, A. Ludi, W. Halg, Inorg. Chem. 19 (1980) 956.
[22] G. Beurskens, G.A. Jeffrey, J. Chem. Phys. 41 (1964) 917.
[23] C.W. Ng, J. Ding, L.M. Gan, J. Solid State Chem. 156 (2001) 400.
[24] H. Tokoro, S. Ohkoshi, T. Matsuda, K. Hashimoto, Inorg. Chem. 43 (2004) 5231.